

Le Retour de Pappus

Richard Evan Schwartz *

December 4, 2024

Abstract

In [S0] we explained how the iteration of Pappus's Theorem gives rise to a 2-parameter family of representations of the modular group into the group of projective automorphisms. In this paper we realize these representations as isometry groups of patterns of geodesics in the symmetric space $X = SL_3(\mathbf{R})/SO(3)$. The patterns have the same asymptotic structure as the geodesics in the Farey triangulation, so our construction gives a 2 parameter family of deformations of the Farey triangulation inside X . We will also describe a bending phenomenon associated to these patterns.

1 Introduction

Pappus's Theorem says that if $A = (A_1, A_2, A_3)$ and $B = (B_1, B_2, B_3)$ consist of collinear points, then so does $C = (C_1, C_2, C_3)$. Starting with the pair (A, B) you produce the pairs (A, C) and (C, B) .

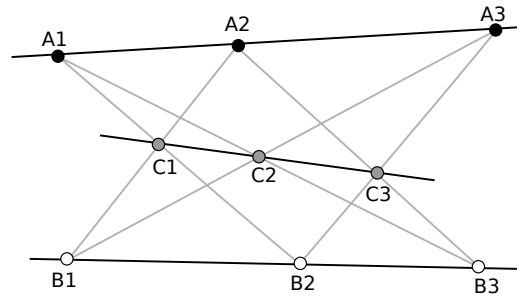


Figure 1.1: Pappus's Theorem

* Supported by N.S.F. Grant DMS-2102802, a Simons Sabbatical Fellowship, and a Mercator Fellowship

In my 1993 paper [S0], I iterate the above construction and then use the result to define a 2 dimensional moduli space of inequivalent representations of the modular group into the group of projective symmetries of the flag variety \mathcal{P} over the projective plane. Here \mathcal{P} is the space of pairs (p, ℓ) where p is a one dimensional subspace in \mathbf{R}^3 , and ℓ is a 2-dimensional subspace in \mathbf{R}^3 , and $p \subset \ell$. Figure 1.2, a concrete example, hints at the limit set of one of these *Pappus modular groups*.

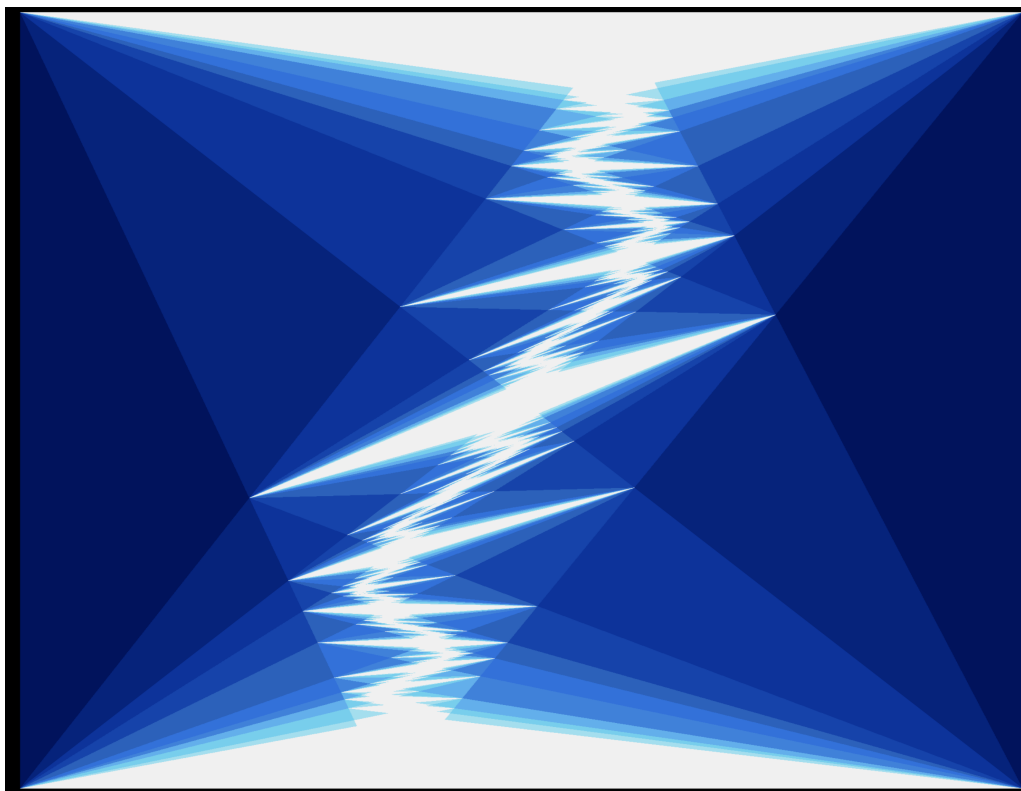


Figure 1.2 A hint of the limit set

The paper [S0] is a precursor of many papers in higher Teichmuller Theory. One can see many of the basic structures in [S0] appearing much more generally e.g. in [Bar], [BCLS], [GW], [KL], and [Lab]. Nowadays, the Pappus modular groups are classified as *relatively Anosov representations in the Barbot component*. Compare [BLV], [KL], and [Bar]. See also [G] and [Hit], two papers roughly contemporaneous with (and even a bit earlier than) [S0], that inspired a huge amount of work in higher Teichmuller Theory.

The purpose of this paper is to give a description of the Pappus modular groups in terms of the associated symmetric space, $X = SL_3(\mathbf{R})/SO(3)$. The description adds another layer of depth and beauty to the Pappus modular groups, and also it is a textbook picture of how a relatively Anosov representation acts on the associated symmetric space as the symmetries of something like a pleated plane. I have wanted to do this for many years, but only recently saw the answer, implicit in [SO, Figure 2.4.2], staring me in the face. See Figure 4.2 below.

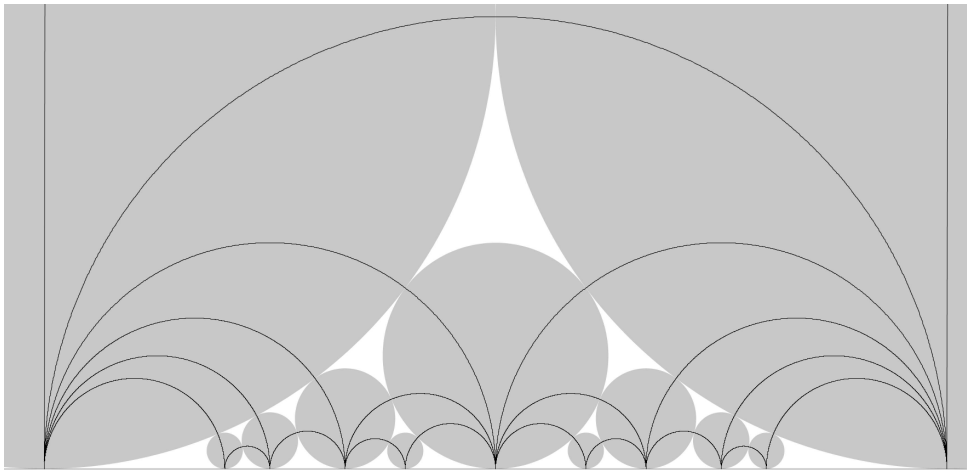


Figure 1.3: Part of the Farey triangulation and dual horodisk packing

Working in the upper half-plane model \mathbf{H}^2 of the hyperbolic plane, one forms a pattern of geodesics by connecting each pair of rational numbers a/b and c/d on the ideal boundary $\mathbf{R} \cup \infty$ by a geodesic if and only if $|ad - bc| = 1$. Here ∞ is interpreted as the fraction $1/0$. The resulting pattern of geodesics is the 1-skeleton of the famous *Farey triangulation*, and the modular group is precisely the group of orientation preserving symmetries of this thing.

The visual boundary ∂X of X is 4-dimensional, and it contains the 3-dimensional \mathcal{P} in a natural way. See §2.4. We say that a *medial geodesic* in X is a geodesic which limits to points in \mathcal{P} at either end. We say that two medial geodesics are *one-end-asymptotic* if, in exactly one direction, they limit on the same flag. We say that they are *non-asymptotic* if they have no ends in common. (Note that in a higher rank symmetric space like X one has distinct geodesics that are asymptotic at both ends.)

Main Result: Let F denote the union of the geodesics in the Farey triangulation. We say that a *Farey pattern* in X is an injective map $\mu : F \rightarrow X$ which is an isometry when restricted to each geodesic of F and which maps pairs of one-end-asymptotic geodesics to pairs of one-end-asymptotic geodesics and pairs of non-asymptotic geodesics to pairs of non-asymptotic geodesics.

Theorem 1.1 *Every Pappus modular group arises as a group of isometries of a Farey pattern. Generically, the Pappus modular group is the full isometry group of the pattern.*

Proof Sketch: A Pappus modular group $\Lambda_{\mathcal{M}}$ is the group of projective symmetries of a certain infinite collection \mathcal{M} of *marked boxes*, objects which encode instances of Pappus's Theorem. Each marked box $M \in \mathcal{M}$ has associated to it a pair of flags $\phi_{M,1}$ and $\phi_{M,2}$ and also an order 2 element $\rho_M \in \Lambda_{\mathcal{M}}$. It turns out that ρ_M , when acting on X , has a unique fixed point p_M . There is a natural 1-parameter family f_M of medial geodesics which foliate a flat in X and limit at their ends to $\phi_{M,1}$ and $\phi_{M,2}$. It turns out that within f_M there is a unique medial geodesic γ_M in f_M which contains p_M . The assignment $M \rightarrow \gamma_M$, as M ranges over \mathcal{M} , gives us the Farey pattern.

The Bending Phenomenon: Let Γ be one of our Farey patterns. Each geodesic in Γ is contained in a unique flat. Our proof that the geodesics of Γ are disjoint will actually show that the associated flats are disjoint as well. Say that a *prism* is a triple of flats corresponding to an ideal triangle in the Farey triangulation. We want to study the geometry of these prisms.

Referring to Figure 1.1, the quantity $|\log(-\chi)|$, where χ is the triple product (as in Equation 10) of the three flags

$$(A_2, \overline{A_1 A_3}), \quad (B_2, \overline{B_1 B_3}), \quad (C_2, \overline{C_1 C_3})$$

gives rise to what we call the *triple invariant* of a Pappus modular group. Compare [FG]. The level sets of the triple invariant give 1-parameter family of Pappus modular groups. Figure 5.3 shows a plot on the character variety.

The geometry of the individual associated prisms associated only depends on the triple invariant. Hence, within such a 1-parameter level set, the prisms are all isometric to each other. As we vary within the level set, we have a bending/shearing phenomenon akin to those found in [T], [P] and [FG]. The geometry of the prisms does not change, but the geometry of pairs of adjacent prisms does change.

An Attempt a Pleated Surface: The Farey patterns typically do not lie in a totally geodesic slice of X . Given the bending phenomenon just discussed, one might wonder whether there is a natural way to fill in around the geodesics to get a kind of pleated surface. In §5.8 I will explain one way to do it, using a coning construction. This gives rise to a piecewise analytic disk with totally geodesic pleats. Some of the pleats are bi-infinite geodesics and some are geodesic rays meeting $\mathbb{3}$ at a time. I do not know how to prove that this disk is embedded, though I guess that it is.

I will also describe how the coning operation gives rise to a kind of filling of the associated prisms, giving something like a pleated $\mathbb{3}$ manifold. I do not know how to prove that this thing is embedded and I don't really see the picture very well. I suspect that I don't have the filling picture in focus yet. Anna Wienhard suggested to me that perhaps the methods in [DR] would do a better job.

The rest of this paper fleshes out the above sketches. In §2 I will explore the geometry of the symmetric space X , explaining it in very elementary terms. In §3 I will exposit large parts of [S0]. To avoid repeating what I already did in [S0], and also benefitting from years of hindsight, I tried to give a more geometric and accessible account here. (See [BLV] for another exposition of [S0] closer to my original one.) In §4 I will put everything together and prove Theorem 1.1. In §5 I will discuss the bending phenomenon and also write down everything else I have figured out about the structure of these patterns in X .

I would like to thank Martin Bridgeman, Bill Goldman, Joaquin Lejtregger, Joaquin Lema, Dennis Sullivan, and Anna Wienhard for various interesting and helpful conversations. I would especially like to thank Martin and the two Joaquins for recently rekindling my interest in the subject.

2 Geometry of the Symmetric Space

2.1 Primer on Projective Geometry

The Projective Plane: The *projective plane* \mathbf{P} is the space of 1-dimensional subspaces of \mathbf{R}^3 . The *affine patch* in \mathbf{P} is the subset consisting of subspaces not contained in the XY -plane. The affine patch is essentially a copy of \mathbf{R}^2 sitting in \mathbf{P} : The subspace containing $(x, y, 1)$ is identified with $(x, y) \in \mathbf{R}^2$.

The Dual Projective Plane: The *dual projective plane* \mathbf{P}^* is the space of 2-dimensional subspaces of \mathbf{R}^3 . A *line* in \mathbf{P} is the set of all 1-dimensional subspaces contained in a fixed 2-dimensional subspace. Thus the lines in \mathbf{P} are in canonical bijection with the points of \mathbf{P}^* .

Projective Transformations: A *projective transformation* is a map of \mathbf{P} induced by an invertible linear transformation. This notion makes sense because linear transformations permute the 1-dimensional subspaces of \mathbf{R}^3 . Projective transformations simultaneously act on \mathbf{P}^* . Projective transformations act as analytic diffeomorphisms on \mathbf{P} and on \mathbf{P}^* . Projective transformations of \mathbf{P} maps lines to lines. The group of projective transformations is 8 dimensional and acts simply transitively on the space of quadruples of general position points in \mathbf{P} . Thus there is a unique projective transformation which takes any given general position quadruple to another given one.

Dualities: A *duality* is a factor-switching map $\delta : \mathbf{P} \cup \mathbf{P}^* \rightarrow \mathbf{P}^* \cup \mathbf{P}$ which maps collinear points to coincident lines. The duality is a *polarity* if it has order 2. A polarity is induced by a quadratic form: Each subspace is mapped to the subspace perpendicular to it with respect to the quadratic form. If this quadratic form is positive definite we call the polarity *definite*. The dot product induces what we call the *standard polarity*, which we call Δ . Any definite polarity has the form $T \circ \Delta \circ T^{-1}$ where T is a projective transformation.

The Flag Variety: The *flag variety* is the subspace of $\mathbf{P} \times \mathbf{P}^*$ consisting of pairs (p, ℓ) where $p \in \ell$. These elements are called *flags*. We call this space \mathcal{P} . The space \mathcal{P} is a 3-dimensional manifold. A projective transformation T and a duality δ act as analytic diffeomorphisms of \mathcal{P} as follows:

$$T(p, \ell) = (T(p), T(\ell)), \quad \delta(p, \ell) = (\delta(\ell), \delta(p)).$$

2.2 Ellipsoids

Frames: We work with unit volume ellipsoids which are centered at the origin in \mathbf{R}^3 . We say that a *frame* is a triple of mutually orthogonal lines through the origin. The *standard ellipsoids* are given by

$$\frac{x^2}{a^2} + \frac{y^2}{b^2} + \frac{z^2}{c^2} = 1, \quad a, b, c > 0. \quad (1)$$

The *standard frame* is the triple of coordinate axes.

We say that the frame f is *associated* to the ellipsoid E if there is an isometry $I \in SO(3)$ such that $I(E)$ is a standard ellipsoid and $I(f)$ is the standard frame. The unit ball has an $SO(3)$ -family of frames associated to it. The generic ellipsoid, e.g. a standard ellipsoid with $a \neq b \neq c$, has a unique associated frame up to permutation of the lines. All other ones, e.g. a standard ellipse with $a = b \neq c$, have an S^1 -family of associated frames.

Principal Lengths: We get the *principal lengths* of an ellipsoid by intersecting it with the lines of any associated frame and taking half the lengths. Thus, the principal lengths of the ellipsoid in Equation 1 are a, b, c .

If the principal lengths of an ellipsoid E are a, b, c we define

$$\lambda(E) = \|V\| = \sqrt{V \cdot V}, \quad V = (\log a, \log b, \log c). \quad (2)$$

Thus $\lambda(E) \geq 0$, with equality if and only if E is the unit ball.

Matrix Representation: Every unit volume ellipsoid has associated to it a unit determinant positive definite symmetric matrix S in the following way. The ellipsoid E_S is the set of vectors v such that $S(v) \cdot v \leq 1$. We say that S *represents* E_S . The identity matrix represents the unit ball. The principal lengths associated to an ellipsoid are the reciprocals of the eigenvalues of the representing matrix.

Group Action: $SL_3(\mathbf{Z})$ acts on the space X of unit volume ellipsoids in the obvious way. If $T \in SL_3(\mathbf{R})$ and $E \in X$, then we have $T(E) \in X$ as well. If the matrix S represents E then the matrix

$$(T^{-1})^t S T^{-1} \quad (3)$$

represents $T(E)$. Here $(\cdot)^t$ is the transpose. To see this, we note that

$$(T^{-1})^t S T^{-1} (T(v)) \cdot T(v) = (T^{-1})^t (S(v)) \cdot T(v) = S(v) \cdot v.$$

2.3 The Symmetric Space

Here we discuss the geometry of the space X of unit volume ellipsoids centered at the origin. We first mention several other interpretations. First, we can think of X as the space of positive definite symmetric matrices of determinant one. As discussed above, each such matrix defines the ellipsoid which is its unit ball. Second, we can think of X as $SL_3(\mathbf{R})/SO(3)$. To see the connection, note that $SL_3(\mathbf{R})$ acts transitively on X and the stabilizer of the unit ball, a distinguished origin in X , is exactly $SO(3)$.

The Metric: The metric d on X can be described as follows.

- $d(ME_1, ME_2) = d(E_1, E_2)$ for any $M \in SL_3(\mathbf{R})$ and $E_1, E_2 \in X$.
- If E_1 is the unit ball then $d(E_1, E_2) = \lambda(E_2)$.

By construction, $SL_3(\mathbf{R})$ acts isometrically on X . It turns out that d is induced by a Riemannian metric of non-positive sectional curvature.

Geodesics through the Origin: Let $E \in X$ be any point other than the unit ball. Let L_1, L_2, L_3 be the lines in an associated frame, and let $\lambda_1, \lambda_2, \lambda_3$ be the corresponding principal lengths. We write $\ell_j = \log(\lambda_j)$. We let $E(t)$ denote the geodesic with the same associated frame and principal lengths $\{\exp(t\ell_j)\}$. By construction, $E(1) = E$. The collection $\{E(t) \mid t \in \mathbf{R}\}$ is a geodesic in X through the origin. The origin is given by $E(0)$. In terms of the matrix representations, there is a 1-parameter subgroup associated to the geodesic defined by E_0 and E , and this subgroup is conjugate in $SO(3)$ to a 1-parameter subgroup of positive diagonal matrices. Every other geodesic in X is carried to a geodesic through the origin by an element of $SL_3(\mathbf{R})$.

Flats A *flat* is a totally geodesic copy of \mathbf{R}^2 embedded in X . The *standard flat* is the union of the points corresponding to the standard ellipsoids. The set of matrices representing the points in the standard flat is exactly the subgroup of positive diagonal matrices. So, the standard flat is the orbit of the origin under the subgroup of positive diagonal matrices. The standard flat has 3 *singular geodesics* through the origin, the ones represented by matrices having repeated eigenvalues. These 3 singular geodesics divide the standard flat into 6 sectors which are called *Weyl chambers*. See Figure 2.1 below. We have this Weyl chamber structure at each point of each flat.

The Basic Involution: Every definite polarity defines an isometry of X with a unique fixed point. Since the definite polarities are all conjugate in $SL_3(\mathbf{R})$ we just have to understand this for the definite polarity Δ induced by the dot product. For any ellipsoid E , the ellipsoid $\Delta(E)$ is the ellipsoid which has the same associated frame as E and reciprocal principal lengths. The matrix representing $\Delta(E)$ is the inverse of the matrix representing E . We can see quite readily that Δ fixes the origin in X and reverses all the geodesics through the origin. Since X is a symmetric space, the geodesic-reversal property implies that Δ acts as an isometry. To be sure, let me give a self-contained proof.

Lemma 2.1 Δ is an isometry of X .

Proof: Let $Y^* = (Y^{-1})^t$ for any $Y \in SL_3(\mathbf{R})$. The map $Y \rightarrow Y^*$ is an order 2 automorphism of $SL_3(\mathbf{R})$.

Let E_0 be the unit ball, as above. Two typical points in $E_1, E_2 \in X$ are given by $M_1(E_0)$ and $M_2(E_0)$ where $M_1, M_2 \in SL_2(\mathbf{R})$. The positive definite symmetric matrix representing E_k is $S_k = M_k^* M_k^{-1}$. The matrix representing $\Delta(E_k)$ is

$$S_k^{-1} = M_k (M_k^*)^{-1} = M_k M_k^t.$$

From this we recognize that $\Delta(E_k) = M_k^*(E_0)$.

From the $SL_3(\mathbf{R})$ -symmetry of the metric, we have

$$d(E_1, E_2) = d(E_0, M_1^{-1}(E_2)) = d(E_0, M_1^{-1}(M_2(E_0))) = \lambda(M_1^{-1}M_2(E_0)).$$

Likewise

$$d(\Delta(E_1), \Delta(E_2)) = \lambda(M_1^t M_2^*(E_0)).$$

It is convenient to set

$$M = M_1^{-1}M_2, \quad S = M^*M^{-1}.$$

With this notation,

$$d(E_1, E_2) = \lambda(M(E_0)), \quad d(\Delta(E_1), \Delta(E_2)) = \lambda(M^*(E_0)).$$

The matrix S represents $M(E_0)$. Because $(*)$ is an automorphism, S^* represents $M^*(E)$. But the eigenvalues of S and the eigenvalues of S^* are reciprocals of each other. Hence $\lambda(M(E_0)) = \lambda(M^*(E_0))$. ♠

2.4 The Visual Boundary

The *visual boundary* of X is the space ∂X of geodesic rays through the origin. Topologically, the visual boundary of X is S^4 , the 4-dimensional sphere. We identify 3 special subsets of the visual boundary:

- The rays corresponding to ellipsoids having principal lengths

$$\lambda^2, 1/\lambda, 1/\lambda,$$

with $\lambda \geq 0$. As $\lambda \rightarrow \infty$, the corresponding ellipsoids look like uncooked spaghetti and they converge to a line through the origin. Thus, the corresponding subset of ∂X is a copy of the projective plane \mathbf{P} .

- The rays corresponding to ellipsoids having principal lengths

$$\lambda, \lambda, 1/\lambda^2,$$

with $\lambda \geq 0$. As $\lambda \rightarrow \infty$, such ellipsoids look like pancakes and they converge to a unique plane through the origin. Thus, the corresponding subset of ∂X is a copy of \mathbf{P}^* .

- The rays corresponding to ellipsoids having principal lengths

$$\lambda, 1, 1/\lambda,$$

with $\lambda \geq 0$. As $\lambda \rightarrow \infty$ the ellipsoids in the same ray look like popsicle sticks and their limit defines a unique flag: The ellipsoids accumulate to a unique line through the origin, one of the lines in the associated frame, and their two largest principle directions pick out a plane, one that is spanned by two of the lines in the associated frame. Thus, the corresponding subset of ∂X is a copy of \mathcal{P} .

Two general geodesic rays in X are *fellow travelers* if there is a uniform bound on the distance between corresponding points on the rays.

Lemma 2.2 *Every geodesic ray in X is the fellow traveler of a geodesic ray through the origin.*

Proof: This is well known. Let γ be such a ray. We have $\gamma = T(\gamma_0)$ where $T \in SL_3(\mathbf{R})$ and γ_0 is a ray through the origin. By symmetry we can assume that γ_0 is a ray in the standard flat.

There are 3 numbers ℓ_1, ℓ_2, ℓ_3 with $\ell_1 + \ell_2 + \ell_3 = 0$ such that the principal lengths of $E_t \in \gamma_0$ is $\exp(t\ell_j)$ for $j = 1, 2, 3$. We order these numbers so that $\ell_1 \geq \ell_2 \geq \ell_3$. Here $t \geq 0$. We associate to γ_0 the standard frame f_0 .

Let L_1, L_2, L_3 be the lines $T(f_0)$. These lines are not necessarily mutually perpendicular. Let $L_1^* = L_1$. Let L_2^* be the line through the origin perpendicular to L_1 inside the span of L_1, L_2 . Let L_3^* be the line through the origin mutually perpendicular to L_1^* and L_2^* . Let E_t^* denote the ellipsoid whose associated frame is (L_1^*, L_2^*, L_3^*) and whose principal lengths are $\exp(t\ell_1), \exp(t\ell_2), \exp(t\ell_3)$. The set $\gamma_* = \{E_t^* \mid t \in \mathbf{R}_+\}$ is a geodesic ray in X through the origin. We want to see that γ and γ^* are fellow travelers.

We can further normalize by an element of $SO(3)$ so that $\gamma_* = \gamma_0$. This is to say that L_1^*, L_2^*, L_3^* are the coordinate axes. Now we want to see that γ_0 and γ are fellow travelers. Consider the diagonal matrix M_t with diagonal entries $\exp(-t\ell_j)$ for $j = 1, 2, 3$. By construction $M_t(E_t^*)$ is the unit ball.

Consider $M_t(E_t)$. This ellipsoid has unit volume and intersects the X -axis in a segment of length 2. We claim that $M_t(E_t)$ intersects the XY -plane in a set of area A_t that is uniformly bounded away from 0 and ∞ . Assuming this claim, $M_t(E_t)$ is uniformly close to the unit ball in shape. Hence $d(M_t(E_t), M_t(E_t^*)) = d(E_t, E_t^*)$ is uniformly bounded.

For the claim, note that E_t intersects L_1 and L_2 respectively in segments of length $2 \exp(t\ell_1)$ and $2 \exp(t\ell_2)$. The first of these numbers is the largest. Also, there is a fixed angle between L_1 and L_2 . Given this situation, we see that E_t intersects L_2^* in a segment of length $2A_t \exp(t\ell_2)$ where $A_t \leq 1$ is uniformly bounded away from 0. Hence $M_t(E_t)$ intersects the XY -plane in a set of area A_t that is uniformly bounded away from 0 and ∞ . ♠

Two distinct geodesic rays through the origin are not fellow travelers. Thus, Lemma 2.2 gives a way to assign a point in ∂X to any geodesic ray. This, in turn, gives a way to extend the action of $SL_3(\mathbf{R})$ to ∂X . This action is compatible with the action of $SL_3(\mathbf{R})$ on each of the sets \mathbf{P} and \mathbf{P}^* and \mathcal{P} . The action of a duality on X also extends to ∂X and is compatible with the action we already have on $\mathbf{P} \cup \mathbf{P}^*$ and \mathcal{P} .

Remark: Consider a *medial ray*, a geodesic ray which is asymptotic to a flag in \mathcal{P} . The ellipsoids look like popsicle sticks far out on the ray. If we apply a linear transformation then, far out on the new ray, the ellipsoids again look like popsicle sticks. This defines the extension more concretely in the special case of interest to us.

2.5 Flats and the Visual Boundary

Now we explain how flats interact with the visual boundary. Consider the standard flat. Each of the 3 singular geodesics through the origin limits in one direction to one of the coordinate axes and in the other direction to the complementary coordinate plane. Thus, the flat has 3 limit points in \mathbf{P} and 3 in \mathbf{P}^* . The 3 geodesics that lie midway between the singular geodesics, all of which are medial geodesics, limit to points in \mathcal{P} . Thus the flat also has 6 limit points in \mathcal{P} . With respect to the circular order on the rays through the origin in the flat, the flag points interlace with the points in \mathbf{P} and \mathbf{P}^* , which are themselves interlaced. Figure 2.1 shows this structure. The limit points in \mathbf{P} and \mathbf{P}^* and \mathcal{P} are respectively denoted by black, white, and grey arrows.

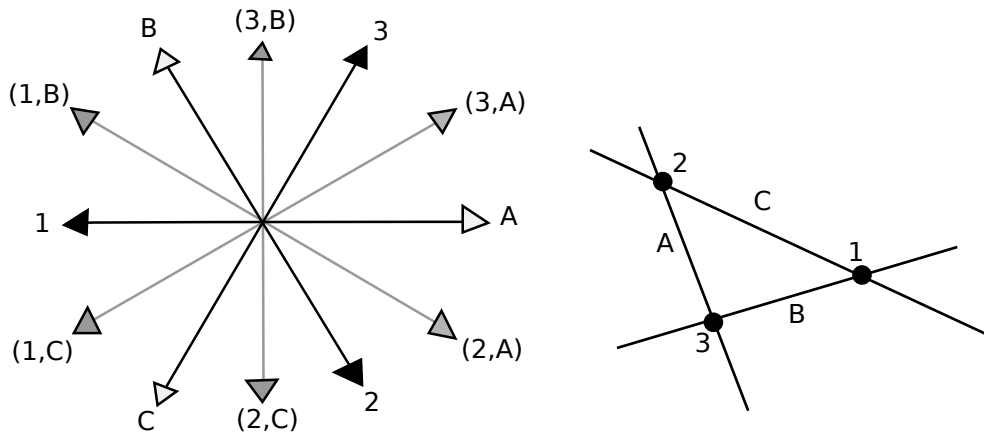


Figure 2.1: The picture in the flat (left) and in \mathbf{P} (right).

This union of 3 points, 3 lines, and 6 flats corresponds naturally to a triangle in \mathbf{P} , and likewise a triangle in \mathbf{P}^* . Here we mean *triangle* in the sense of the points and lines. The complement of our line triple in \mathbf{P} is a union of 4 open 2-dimensional triangular faces. We ignore these faces.

Every point of every flat in X has the structure described above. In particular, each flat defines a triangle in \mathbf{P} (in the sense above). Conversely every triangle in \mathbf{P} comes from a flat in this way. In short, the flats are naturally in bijection with the triangles in \mathbf{P} .

3 The Pappus Modular Groups

3.1 Actions on the Farey Graph

Let Γ be the set of oriented geodesics in the Farey graph. To each directed geodesic in Γ we associate the halfplane it bounds that a person walking along the geodesic would see on their right.

There are 3 permutations of Γ . Let e be some oriented geodesic in γ . We define $i(e)$ to be the same geodesic but with the opposite orientation. The operations t and b are such that the geodesics $i(e)$, $t(e)$, and $b(e)$ are the edges of an ideal triangle in the Farey graph, and they are oriented counterclockwise around the triangle. Figure 3.1 shows how these operations act on a typical edge e . We also shade the associated halfplanes.

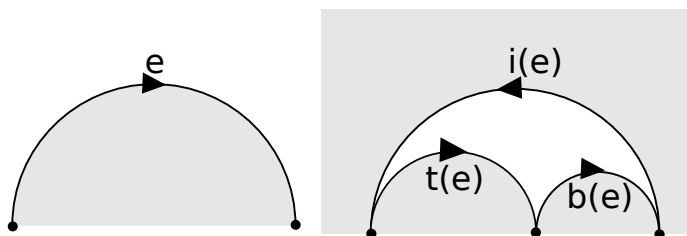


Figure 3.1: The operations t and b .

The halfplanes associated to $t(e)$ and $b(e)$ are contained in the halfplane associated to e . The halfplanes associated to $i(e)$ and $t(e)$ and $b(e)$ are disjoint. The operations above satisfy the following relations.

$$tit = b; \quad bib = t, \quad tibi = I, \quad biti = I, \quad (it)^3 = (ib)^3 = I. \quad (4)$$

Here I is the identity permutation.

From these relations, and from the nesting properties of the halfplanes, we see that the group of permutations generated by (i, t, b) is isomorphic to the modular group, namely the free product $\mathbf{Z}/2 * \mathbf{Z}/3$. Concretely, the group in question is generated by i and it , elements of order 2 and 3 respectively.

This action of the modular group on Γ is completely combinatorial. At the same time there is a second action of the modular group on Γ , namely the group of orientation preserving hyperbolic isometries. This copy of the modular group is generated by an order 3 rotation of any of the ideal triangles, and an order 2 element which stabilizes an edge and reverses its direction. These two actions commute. Thus we have 2 commuting modular group actions on Γ , one combinatorial and one geometrical.

3.2 Convex Marked Boxes

Our description will depart from that in [S0] though not in an essential way. We identify the affine patch of \mathbf{P} with \mathbf{R}^2 . We fix a square $Q \subset \mathbf{R}^2$ whose sides have unit length and are parallel to the coordinate axes. We think of Q as a solid square.

Model Convex Marked Boxes: We say that a *model convex marked box* is a triple (Q, t, b) where t is a point in the interior of the top edge of Q and b is a point in the interior of the bottom edge of Q . We will often abbreviate this terminology to *model box*.

Convex Marked Boxes: We say that a *convex marked box* is a triple (Q', t', b') which is projectively equivalent to some model convex marked box. That is, there is a projective transformation Ψ such that

$$(Q', t', b') = \Psi(Q, t, b).$$

We call the edge of Q' containing t' the *top edge*. We call the edge of Q' containing b' the *bottom edge*. See Figure 3.2 below.

Reflection Ambiguity: Note that there are two model convex marked boxes projectively equivalent to a general convex marked box. Let ρ denote the reflection in the vertical midline of Q . Then $\rho(Q, t, b)$ is another model convex marked box and $\Psi \circ \rho$ is another projective transformation, and

$$(Q', t', b') = (\Psi \circ \rho)(\rho(Q, t, b)).$$

We call this the *reflection ambiguity*. Up to reflection ambiguity, each convex marked box is projectively equivalent to a unique model convex marked box.

The Box Invariant: We let x denote the distance from t to the top left vertex of Q and we let y denote the distance from b to the bottom right vertex of Q . With the reflection ambiguity above in mind, we write $(x, y) \sim (1 - x, 1 - y)$. To the marked box (Q, t, b) we associate the (\sim) equivalence class $[(x, y)]$. We call this the *box invariant*.

We extend the box invariant to all other convex marked boxes by symmetry. By construction, two convex marked boxes are equivalent via a projective transformation if and only if they have the same box invariant. The box invariant can also be computed using cross ratios, as we discuss in §3.4.

3.3 The Box Operations

Now we imitate what we did for the oriented Farey graph.

There are 3 operations on convex marked boxes, which we call i , t , and b . Figure 3.2 shows these operations on a marked box M . The operations t and b encode Pappus's theorem.

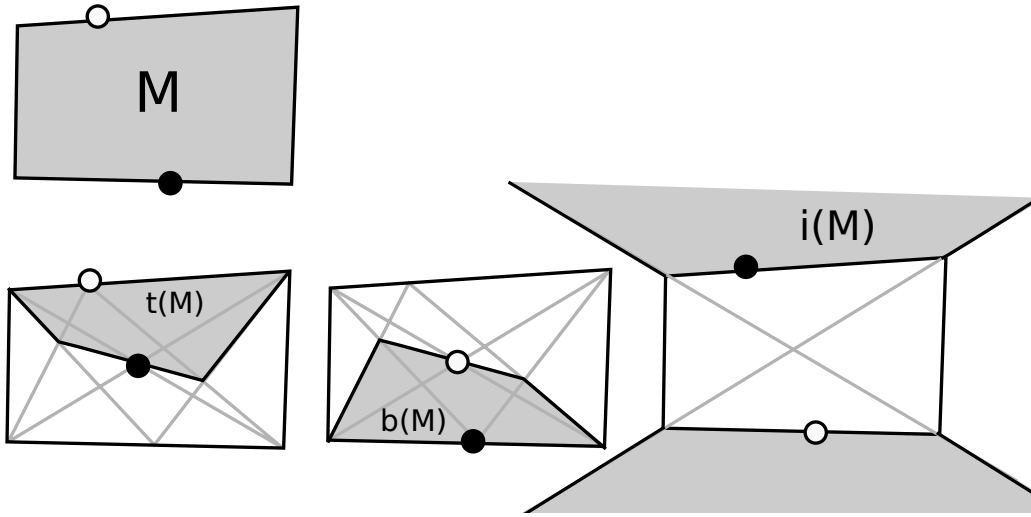


Figure 3.2: The operations t, b, i on the convex marked box M .

On the right hand side, the top of $i(M)$ is the bottom of M and the top of $i(M)$ is the bottom of M . The top vertices in each case are colored white and the bottom ones are colored black. The box $i(M)$ looks unbounded in the affine patch, but is indeed a convex marked box in \mathbf{P} . The shading is meant to go on forever, so to speak, but we can of course only draw part of it.

The nesting properties of the marked boxes are the same as for the operations on the oriented Farey graph. Moreover, one can check easily, by drawing the relevant lines, that the relations in Equation 4 hold. The calculations are done out in [S0]. From the relations in Equation 4 and from the nesting properties, we see that the group generated by i, t, b is isomorphic to $\mathbf{Z}/2 * \mathbf{Z}/3$ as above. Thus we have a combinatorial modular group operation on the space of convex marked boxes.

3.4 A Box Invariant Calculation

In this section we will start with the model box M with invariant $[(x, y)]$ and then compute the box invariants for $t(M)$ and $b(M)$. Given four collinear points $a, b, c, d \in \mathbf{P}$ have a *cross ratio*

$$[a, b, c, d] = \frac{(a - b)(c - d)}{(a - c)(b - d)} = \text{any defined entry of } \frac{(a \times b)(c \times d)}{(a \times c)(b \times d)} \quad (5)$$

We implement the first formula by identifying the line containing a, b, c, d with the X -axis by a projective transformation. The answer we get is independent of the choices made. The second formula is how we actually do our computations. It applies when the points a, b, c are represented by vectors in \mathbf{R}^3 – i.e., given in terms of homogeneous coordinates. We take the 4 cross products and then multiply and divide them pointwise. Each well-defined entry equals $[a, b, c, d]$. The cross ratio of 4 coincident lines has a similar definition..

For the big box in Figure 3.3 (with corners s, u, a, c) the box invariant is $[(x, y)]$ where

$$x = [s, t, u, \zeta], \quad y = [a, b, c, \zeta], \quad \zeta = \overline{su} \cap \overline{ca}.$$

This projectively natural formula works for any marked box. We name points in Figure 3.3 by vectors in \mathbf{R}^3 that represent them.

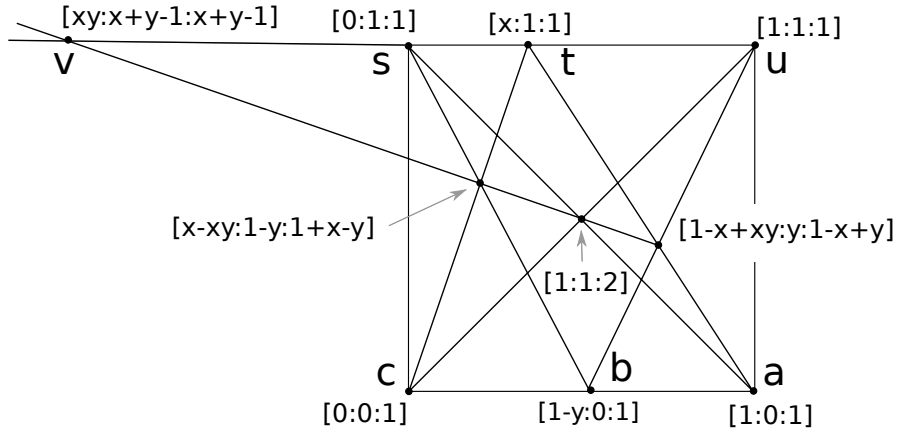


Figure 3.3: The relevant coordinates

A calculation shows $t(M)$ and $b(M)$ both have box invariant $[(1 - y, x)]$. For instance $[s, t, u, v] = 1 - y$, and this calculates the first entry in the box invariant for $t(M)$.

3.5 Projective Symmetries of an Orbit

Let M be any marked box.

Lemma 3.1 *There is an order 3 projective transformation T with the action $t(M) \rightarrow b(M) \rightarrow i(M)$.*

Proof: Since $t(M)$ and $b(M)$ have the same box invariant, there is a projective transformation T such that $T(t(M)) = b(M)$. Since the operations commute with projective transformations, the relations in Equations 4 give us

$$T(b(M)) = T(tit(M)) = tiT(tM) = tib(M) = i(M).$$

$$T(i(M)) = T(tib(M)) = tiT(b(M)) = tii(M) = t(M).$$

The fact that $T^3(M) = M$ forces T^3 to be the identity. ♠

Lemma 3.1 gives us a $\mathbf{Z}/3 * \mathbf{Z}/3$ geometric action, by projective transformations, on each convex marked box orbit. The generators can be taken as ib and it . This group $\langle it, ib \rangle$ has index 2 in the modular group. What is missing is a symmetry that maps M to $i(M)$.

3.6 Doppelgangers

Lemma 3.1 implies that $i(M)$ also has box invariant $[(1 - y, x)]$. This is different from the box invariant $[(x, y)]$ of M . For this reason, M and $i(M)$ are typically not projectively equivalent. It turns out that there is a polarity which maps M to $i(M)$. To make sense of this statement we first need to interpret marked boxes in a way that is compatible with the action of dualities. Our treatment here departs somewhat from that in [S0] but not in essential ways.

We can specify a convex marked box as a 6-tuple of points (s, t, u, a, b, c) . These points go in cyclic order around the boundary of the convex quadrilateral. Figure 3.4 (left) shows what we mean. The data (u, t, s, c, b, a) describes the same convex marked box. Thus it is really the pair of these 6-tuples which describes the marked box.

Figure 3.4 (right) shows a collection of 6 lines, (S, T, U, A, B, C) . This data carries the same information as (s, t, u, a, b, c) and one can recover point list from the line list and *vice versa*. We call these two lists *dopplegangers*.

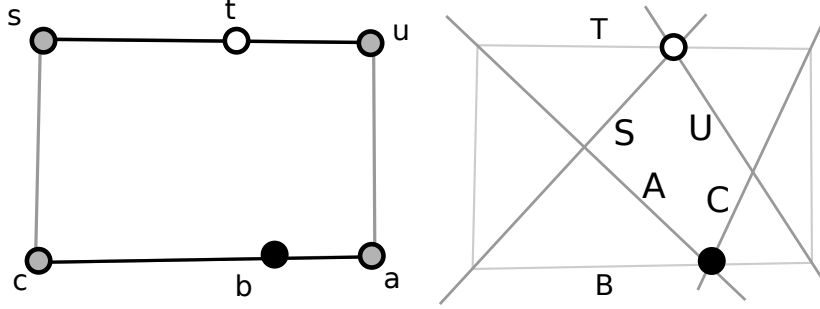


Figure 3.4: A convex marked box and its doppelganger

Lemma 3.2 (Duality) *Let δ be a duality. The ordered list*

$$(\delta(S), \delta(T), \delta(U), \delta(A), \delta(B), \delta(C))$$

is the data associated to a convex marked box.

Proof: The data we are considering has the right form for describing a convex marked box: namely 6 points contained in triples on a pair of lines. The issue is the convexity.

We first discuss a geometric criterion for convexity that will be easier to work with. Let

$$x = \overline{su} \cap \overline{ac} = T \cap B. \quad (6)$$

The points (s, t, u, x) and (a, b, c, x) are both interlaced on the straight lines which contain them. That is, s, u separates t, x on the line \overline{su} and a, c separates b, x on the line \overline{ac} . This property is a necessary and sufficient condition for convexity because, when we normalize so that s, u, a, c are the vertices going cyclically around our unit square, the interlacing property puts t and b respectively on the top and bottom edges of the unit square.

Now we go back to the the doppelganger. Define

$$X = \overline{(S \cap U)(A \cap C)} = \overline{tb}. \quad (7)$$

The lines S, T, U, X are interlaced on the circle defined by the pencil of lines through t . Likewise the lines A, B, C, X are interlaced on the pencil of lines through b . When we apply the polarity we get the needed interlacing for convexity. ♠

Given the convex marked box M in \mathbf{P} described by (s, t, u, a, b, c) , we let M^* be the convex marked box in \mathbf{P}^* described by (S, T, U, A, B, C) . We call

M and M^* *dopplegangers*. It makes sense to perform the operations i, t, b in \mathcal{P}^* . We just interchange the roles played by points and lines.

Lemma 3.3 (Compatibility) *Suppose M and M^* are dopplegangers and γ is one of the three marked box operations. Then $\gamma(M)$ and $\gamma(M^*)$ are dopplegangers.*

Proof: We keep the notation from above. Consider the operation i . The data for the marked box $i(M)$ is (a, b, c, u, t, s) and the data for the marked box $i(M^*)$ is (A, B, C, U, T, S) . In terms of the data, these are purely combinatorial operations. From this we can see that $i(M)$ and $i(M^*)$ are dopplegangers.

Now we consider the operation t (not to be confused with one of the vertices of our data.) The data for $t(M)$ is given by (s, t, u, a', b', c') , where

$$a' = \overline{ta} \cap \overline{ub}, \quad b' = \overline{sa} \cap \overline{uc}, \quad c' = \overline{tc} \cap \overline{sb}.$$

The data for $t(M^*)$ is given by (S, T, U, A', B', C') , where

$$A' = \overline{(T \cap A)(U \cap B)} \quad B' = \overline{(S \cap A)(U \cap C)} \quad C' = \overline{(T \cap C)(S \cap B)}.$$

Figure 3.5 shows the construction.

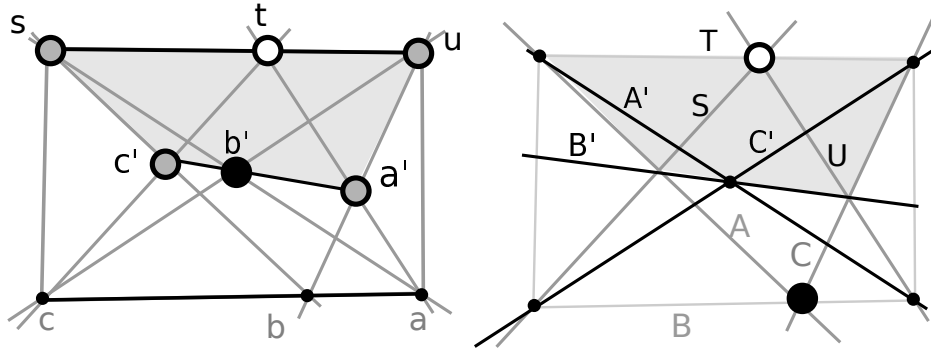


Figure 3.5: The effect of the operation t .

Looking at these formulas and inspecting the data, we see that $t(M)$ and $t(M^*)$ are dopplegangers. A similar argument works for the operation b . ♠

3.7 Duality

We say that an *enhanced box* is a pair (M, M^*) of doppelgangers. If we have a duality δ and an enhanced box (M, M^*) then we define

$$\delta((M, M^*)) = (\delta(M^*), \delta(M)). \quad (8)$$

In this way, dualities also act on (enhanced) marked box orbits. Now we now come to the heart of the matter.

Lemma 3.4 *The boxes $i(M)$ and M^* have the same box invariants.*

Proof: Let us change our notation so that M has box invariant $[(\alpha, \beta)]$. Let x and X be as in Equations 6 and 7. We have $\alpha = [s, t, u, x]$ and $\beta = [a, b, c, x]$. We have already seen that $i(M)$ has box invariant $[(1 - \beta, \alpha)]$.

We compute the box invariant of M^* by taking cross ratios of the relevant lines. Looking at Figure 3.4, we see that M^* has box invariant $[(\beta, 1 - \alpha)]$ because $[S, T, U, X] = [c, x, a, b] = \beta$ and $[A, B, C, X] = [u, t, s, x] = 1 - \alpha$. ♠

Lemma 3.5 *There is a polarity which maps $i(M)$ to M^* .*

Proof: For ease of notation we write iM for $i(M)$. Since iM and M^* have the same box invariants, there is some duality δ such that $\delta(iM) = M^*$. But then, simultaneously,

$$\delta((iM)^*) = M^{**} = M.$$

This fact, together with the Compatibility Lemma, gives us

$$\delta(M^*) = \delta(iiM^*) = i\delta(iM^*) = \delta((iM)^*) = iM.$$

This shows that $\delta^2(M) = M$. But then δ is a polarity. ♠

Each convex marked box orbit defines a unique enhanced box orbit on which the group $\mathbf{Z}/2 * \mathbf{Z}/3 = \langle i, t, b \rangle$ acts. If we forget the doppelgangers we just get the original orbit.

Lemma 3.5 combines with Equation 8 to give us the missing symmetry. Now we know that there is a polarity that interchanges M and $i(M)$ for every enhanced box M in the orbit. Combining Lemmas 3.1 and 3.5, we get

a geometric modular group action on each enhanced box orbit. These are the Pappus modular groups.

Once we single out some enhanced box in the orbit we get a natural map from the oriented geodesics in the Farey graph to the enhanced box orbit. The natural map intertwines the two commuting modular group actions on the oriented Farey graph and the two commuting modular group actions on the enhanced box orbit. The order 3 isometric rotations of the ideal triangles in the Farey triangulation correspond to the projective transformations from Lemma 3.1, and the order 2 edge stabilizers acting on the Farey graph correspond to the polarities from Lemma 3.5. Theorem 1.1 makes this intertwining map more canonical and meaningful.

3.8 Discussion

Our marked box operations make sense over essentially any field. (Fields over $\mathbf{Z}/2$ do not have enough points on a line to make sense of the constructions.) In particular, the convexity assumptions are not really crucial for Equation 4. We needed the convexity to guarantee that these operations generate a faithful action of the modular group. For instance, over finite fields, the action could not possibly be faithful.

The projective symmetry proofs in Lemmas 3.1 and 3.5 would also work over essentially any field. They are really algebraic arguments, and our pictures are just a guide to the calculations. In this sense, our arguments here are more robust than the arguments given in [S0]. We gave picture proofs of Lemma 3.1 and Lemma 3.5 in [S0] which seem to rely on the real field.

One disadvantage of our proof of Lemma 3.5 is that it does not recognize the polarity as a definite polarity. In the next chapter we will revisit the argument in [S0] and show that the polarity in Lemma 3.5 is a definite polarity. Thus, the next chapter contains a second proof of Lemma 3.5.

In the case at hand, we could get the definite nature of the polarity just from homotopy considerations. We could check, in a single case, that the polarity was definite and then we would argue by continuity that all the polarities that arise from marked boxes are definite.

4 The Symmetric Space Picture

4.1 Recognizing the Standard Polarity

Recall that the standard polarity Δ is the one induced by the usual dot product. In this section we explain how the standard polarity acts on points and lines in the affine patch.

Figure 4.1 shows L and $\Delta(L)$ when L is a line that intersects the unit circle C . Working in an affine patch, we have $\Delta(L) = -p$, where p is the intersection of the tangent lines through the points of $L \cap C$. The points p and q satisfy the *reciprocity condition*: $\|p\|\|q\| = 1$. Here $\|p\|$ is the distance from p to the origin in \mathbf{R}^2 . This means also that $\| -p\|\|q\| = 1$.

The action of Δ on all other lines is determined by the action of Δ on the lines which intersect C . If L is disjoint from C then $\Delta(L)$ is a point contained in the unit disk. The same kind of reciprocity result about the relevant distances to the origin holds in this case as well. To give an extreme case, Δ maps the line at ∞ to the origin.

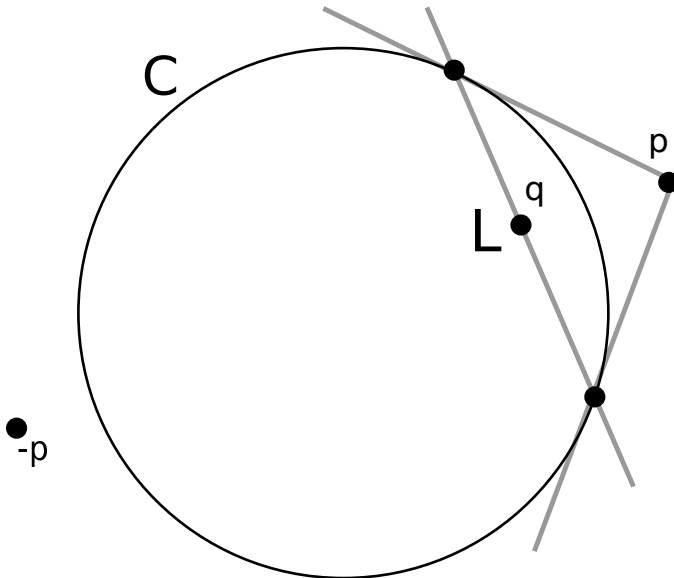


Figure 4.1: A geometric picture of the standard polarity

We have described the action of Δ on lines, but the action on lines determines the action on points. Indeed, Δ is a polarity, a map of order 2. So, the action of Δ on lines immediately determines the action of Δ on points.

4.2 Another View of the Polarity

Now we revisit Lemma 3.5. Figure 4.2, an elaboration of [S0, Figure 2.4.2], shows how we normalize the marked box M so that Δ maps M to $i(M)$. The lines T and B go through the origin in \mathbf{R}^2 . The points t and b lie at ∞ on these lines. We also have $\|a\|\|c\| = \|u\|\|s\| = 1$. The shaded regions show the convex quadrilaterals (in \mathbf{P}) comprising M and $i(M)$ respectively.

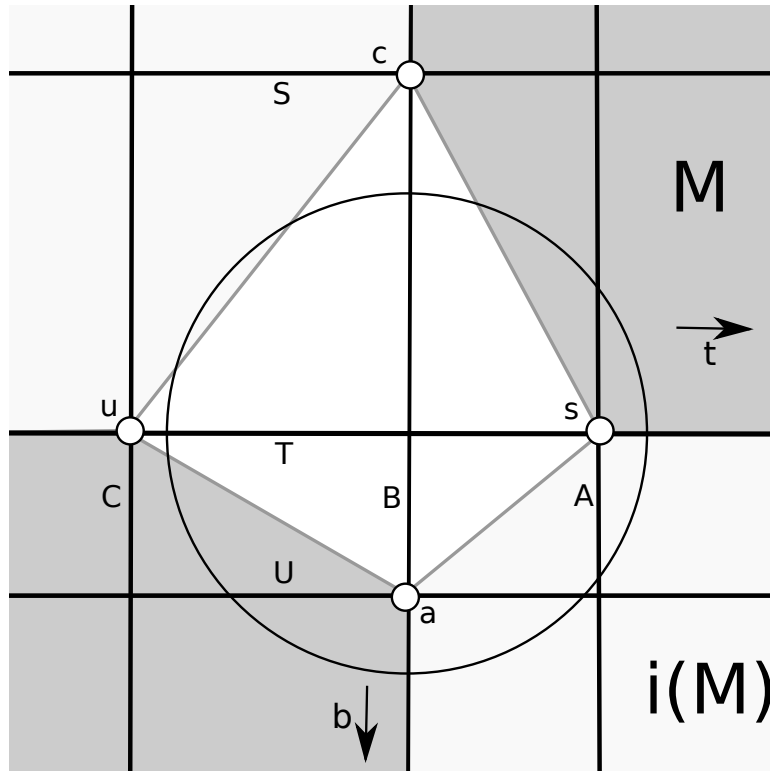


Figure 4.2: A normalized view of M and $i(M)$.

Comparing Figures 4.1 and 4.2 we see that Δ has the action

$$(s, t, u, a, b, c) \rightarrow (C, B, A, S, T, U) = i(S, T, U, A, B, C).$$

Thus Δ maps M to $i(M)$ as claimed.

By symmetry, there is a definite polarity which maps each marked box M to the marked box $i(M)$. This shows that the polarity in Lemma 3.5 is a definite polarity.

4.3 The Farey Patterns

Let \mathcal{M} be a marked box orbit and let $\Lambda_{\mathcal{M}}$ be the Pappus modular group of projective symmetries of \mathcal{M} . For each marked box M of \mathcal{M} we have a definite polarity $\delta_M \in \Lambda_{\mathcal{M}}$ which swaps M and $i(M)$. We let $p_M \in X$ be the fixed point of δ_M . Equivalently, p_M is the unit volume ellipsoid for the quadratic form which gives δ_M .

Note that $p_{i(M)} = p_M$. The points in X we have just constructed correspond to the fixed points of the order 2 elements of $\Lambda_{\mathcal{M}}$. There is also a flat f_M we can associate to the marked box M . Let (t, T) be the top flag of M and let (b, B) be the bottom flag. We have a triangle in \mathbf{P} whose vertices are $(t, b, T \cap B)$ and whose sides are (T, B, \overline{tb}) . The flat f_M is the flat associated to this triangle, as discussed in §2.3.

Lemma 4.1 *We have $p_M \in f_M$.*

Proof: By symmetry, it suffices to consider the case when M is normalized as in Figure 4.2. In this case $\delta_M = \Delta$ and p_M is the origin in X , the point which names the unit ball in \mathbf{R}^3 . The triangle is the one defined by the coordinate axes and coordinate planes. Thus the flat f_M is the standard flat. In this case f_M , the standard flat, contains the origin p_M of X . ♠

We can also associate to M a 1-parameter subgroup of $SL_3(\mathbf{R})$. Consider the set of matrices whose eigensystem is

$$(\lambda, 1/\lambda, 1), \quad (t, b, T \cap B), \quad \lambda \in \mathbf{R}. \quad (9)$$

This set forms a 1-parameter subgroup H_M of $SL_3(\mathbf{R})$ which acts as translation on f_M . When M is normalized as in Figure 4.2, the matrices are diagonal, with diagonal entries $\lambda, 1/\lambda, 1$. The orbits of H_M in f_M give a foliation of f_M by medial geodesics which limit on one end to the flag (t, T) and on the other end to (b, B) . There is a unique member of this foliation which contains p_M . This is the medial geodesic we associate to M . We call it γ_M . We choose the orientation so that γ_M is asymptotic to (t, T) in the backwards direction and asymptotic to (b, B) in the forwards direction.

Definition: Let $\Gamma_{\mathcal{M}}$ denote the union of all the oriented geodesics of the form γ_M for $M \in \mathcal{M}$.

This is our pattern of geodesics in X corresponding to the Pappus modular group $\Lambda_{\mathcal{M}}$. Since the geodesics in $\Gamma_{\mathcal{M}}$ are bijectively associated with marked boxes in \mathcal{M} , it makes sense to speak of the combinatorial modular group action on $\Gamma_{\mathcal{M}}$.

Once we have chosen a single oriented geodesic $\gamma \in \Gamma$ and a single oriented geodesic $\gamma_M \in \Gamma_M$ we have a canonically defined bijection $\Gamma \rightarrow \Gamma_M$ which has the following virtues:

- The bijection is an isometry on each geodesic.
- The bijection intertwines the two combinatorial modular group actions.
- The bijection intertwines the two geometric modular group actions.

Lemma 4.2 *Two geodesics in Γ_M are asymptotic if and only if the corresponding geodesics are asymptotic in Γ .*

Proof: Given the nesting properties of the convex quads underlying our marked boxes in \mathcal{M} we see that two flags associated to boxes in \mathcal{M} coincide if and only if the corresponding rational points in $\mathbf{R} \cup \infty$ are the same. Our lemma follows from this fact, and from the construction of the geodesics in Γ_M . ♠

One of the basic results we proved in [S0] is that the flags associated to the marked boxes in \mathcal{M} are dense in a continuous loop in \mathcal{P} . Typically this is a fractal loop, as Figure 1.2 suggests. Our bijection between geodesics in the Farey triangulations and geodesics in Γ_M induces a homeomorphism from $\mathbf{R} \cup \infty$ to this loop.

There is one special case where the underlying marked boxes are *symmetric*. In this case the marked box has fixed by an order 2 reflection which fixes a point p and a line ℓ . The box invariants in this case are $(1/2, 1/2)$. In this case, the Pappus modular group stabilizes a totally geodesic copy of \mathbf{H}^2 sitting in X . The corresponding loop in \mathcal{P} consists of all the flags whose points lie on ℓ and whose lines contain p .

In the symmetric case, the corresponding Farey pattern is isometric to the usual Farey triangulation. This symmetric case just recreates an isometric copy of the Farey pattern in X . As we move away from the symmetric case, we get nontrivial deformations of the Farey pattern.

4.4 Symmetry

In this section we analyze the symmetry of our Farey pattern. Let $\Lambda_{\mathcal{M}}$ denote the Pappus modular group associated to the marked box orbit \mathcal{M} . Let $\widehat{\Lambda}_{\mathcal{M}}$ denote the symmetry group of the Farey pattern $\Gamma_{\mathcal{M}}$. This is the subgroup of isometries which preserve the pattern.

Lemma 4.3 $\Lambda_{\mathcal{M}} \subset \widehat{\Lambda}_{\mathcal{M}}$.

Proof: Note that γ_M and $\gamma_{i(M)}$ are the same geodesic but with opposite orientations. δ_M is an isometry of the underlying geodesic and just reverses the orientation. Thus δ_M swaps γ_M and $\gamma_{i(M)}$. Given the naturality of our construction, $\gamma \in \widehat{\Lambda}_{\mathcal{M}}$. Also given the naturality of our construction, the order 3 projective transformation T whose orbit is $i(M) \rightarrow t(M) \rightarrow b(M)$ preserves the corresponding union of 3 oriented geodesics in $\Gamma_{\mathcal{M}}$. The same naturality shows that $T \in \widehat{\Lambda}_{\mathcal{M}}$. Since $\Lambda_{\mathcal{M}}$ is generated by the order 2 and order 3 elements, $\Lambda_{\mathcal{M}} \subset \widehat{\Lambda}_{\mathcal{M}}$. ♠

Lemma 4.4 For a generic marked box orbit \mathcal{M} , we have $\Lambda_{\mathcal{M}} = \widehat{\Lambda}_{\mathcal{M}}$.

Proof: A *Farey triangle* in $\Gamma_{\mathcal{M}}$ is a triple of unoriented medial geodesics in the Farey pattern which correspond to the boundary of an ideal triangle in the Farey triangulation. Given the asymptotic properties of geodesics in the Farey pattern, every isometry of $\Gamma_{\mathcal{M}}$ permutes the Farey triangles.

Suppose we have an isometry ψ of X which preserves $\Gamma_{\mathcal{M}}$. Since $\Lambda_{\mathcal{M}}$ acts transitively on the oriented medial geodesics in our pattern, we can assume without loss of generality that ψ stabilizes some oriented medial geodesic $\gamma_{i(M)}$ in the pattern. Since $\Lambda_{\mathcal{M}}$ has a polarity reversing the orientation of this geodesic, we can assume without loss of generality that ψ is a linear transformation which stabilizes the unoriented geodesic in the pattern which is asymptotic to the two flags (t, T) and (b, B) . Here (t, T) and (b, B) respectively are the top and bottom flags associated to the marked box M .

Consider the fourth power ψ^4 . This element must stabilize the oriented geodesic γ_M and also each of the two Farey triangles which involve γ_M . In terms of the projective action of ψ^4 on \mathbf{P} , this element must fix the 3 points $(t, b, T \cap B)$ and also the 4th point w_1 which is common to both $b(M)$ and $t(M)$. The point I mean is simultaneously the top point of $b(M)$ and the

bottom point of $t(M)$. Generically these 4 fixed points are in general position, and this forces ψ^4 to be the identity.

To get a finer analysis, we normalize M as in Figure 4.2. Once we do this, we see that ψ permutes two points at infinity (meaning in $\mathbf{P} - \mathbf{R}^2$ and hence ψ preserves the affine patch \mathbf{R}^2 . Also, ψ permutes the coordinate axes in \mathbf{R}^2 . These facts, together with the fact that ψ has finite order, forces ψ to act as an isometry of \mathbf{R}^2 .

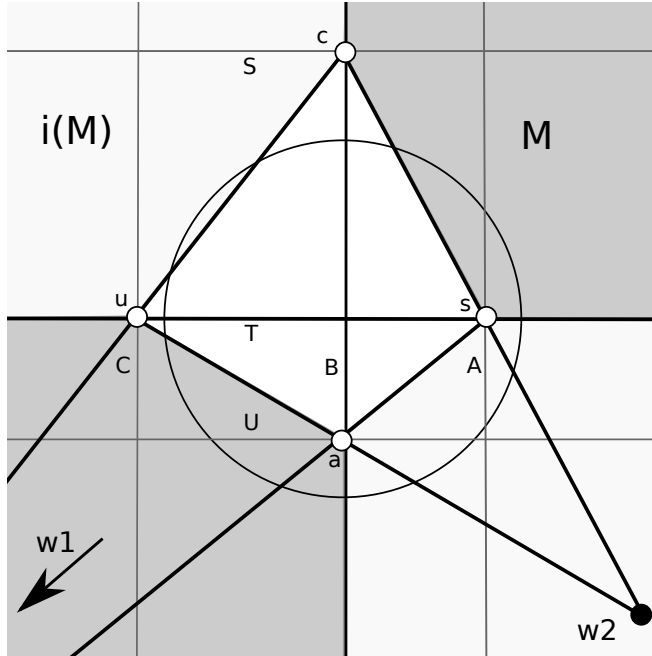


Figure 4.3 The points w_1 (off screen) and w_2 .

Consider the two points

$$w_1 = \overline{cu} \cap \overline{as}, \quad w_2 = \overline{au} \cap \overline{cs}.$$

The point w_1 is the point common to $b(M)$ and $t(M)$ and the point w_2 is the point common to $bi(M)$ and $ti(M)$. These points correspond to the limit points of the two abovementioned Farey triangles which are opposite γ_M . The element ψ must either preserve or permute these two points. Generically, they are not the same distance from the X -axis (or from the Y -axis) and so ψ must preserve them. But then the same argument as above shows that ψ is the identity. So, for a generic choice of \mathcal{M} we have $\Lambda_{\mathcal{M}} = \hat{\Lambda}_{\mathcal{M}}$. ♠

4.5 Disjointness

To finish the proof of Theorem 1.1 we need to show that every two distinct geodesics γ_{M_1} and γ_{M_2} in or pattern $\Gamma_{\mathcal{M}}$ are disjoint. We write $\gamma_1 = \gamma_{M_1}$, etc. We will prove the stronger result that the flats f_1 and f_2 are disjoint in all cases.

Lemma 4.5 *If M_1 and M_2 share a common flag then the flats f_1 and f_2 are disjoint.*

Proof: Suppose that f_1 and f_2 intersect. We can normalize so that this intersection point is the origin in X . Then f_1 and f_2 are two geodesics through the origin that define the same point on ∂X in one direction. This forces $f_1 \cap f_2$ to contain a medial geodesic. But then both flats are determined by the same pair of flags and hence coincide. We are really invoking the more general principle that distinct flats can only share a geodesic if it is one of the singular geodesics. ♠

It remains to consider the case when M_1 and M_2 have no flags in common. The convex quadrilaterals underlying M_1 and M_2 are, like the halfplanes associated to the Farey triangulation, either nested or disjoint. Since we have $f_{M_j} = f_{i(M_j)}$ we can replace M_j by $i(M_j)$ if necessary and then assume that M_1 and M_2 have nested underlying convex quadrilaterals Q_1 and Q_2 .

Suppose for the sake of contradiction that f_1 and f_2 intersect. We can normalize so that the intersection point is the origin in X and that f_1 is the standard flag. We can further normalize so that H_1 is the subgroup of diagonal matrices with entries $(\lambda, 1/\lambda, 1)$. The box M_1 almost looks like the box M in Figures 4.2 and 4.3. The only difference is that the reciprocity condition is gone. That is, M_1 is the image of M under a positive diagonal linear transformation acting on \mathbf{R}^2 . The important thing is that the top and bottom lines of M_1 are the coordinate axes in \mathbf{R}^2 .

Consider the triangle τ_2 associated to f_2 . Since f_2 contains the origin in X , the triangle τ_2 is *orthogonal* in the sense that the three 1-dimensional subspaces representing its vertices are mutually orthogonal. Equivalently, τ_2 is invariant under the standard polarity Δ . This is to say that Δ maps each point of the triangle to the opposite line defined by the triangle.

Define the *positive cone* in \mathbf{R}^2 to be the interior of the union of the $++$ and $--$ quadrants. The important thing about M_1 is that its top and bottom lines cut out the positive cone.

Lemma 4.6 *Two of the lines defined by τ_2 have negative slope.*

Proof: Any convex quadrilateral strictly contained in the convex quad Q_1 associated to M_1 lies in the positive cone. Since M_1 and M_2 have no flags in common, and $Q_2 \subset Q_1$, we see that Q_2 lies in the positive cone. This means that the top and bottom points of Q_2 are contained in the positive cone.

Let p be one of the points of τ_2 in the positive quadrant. The line of τ_2 opposite to p is the image $\Delta(p)$. Given the action of Δ depicted in Figure 4.1, we see that $\Delta(p)$ has negative slope. The extreme cases happen when p is near one of the two coordinate axes. In these cases, the slope of $\Delta(p)$ is near 0 or ∞ . So, if p_1 and p_2 both lie in the positive quadrant then $\Delta(p_1)$ and $\Delta(p_2)$ have negative slope. ♠

The top line and bottom line of M_2 (meaning the lines that extend the top and bottom edges of Q_2) are two of the three lines of τ_2 . By Lemma 4.6, at least one of them has negative slope. We will contradict this by showing that both these lines have non-negative slope.

Let S_1 denote the union of the two edges of the Q_2 which are not the top or bottom edge. The sides of S_1 are the side edges.

Lemma 4.7 *The top and bottom lines of M_2 intersect both segments of S_1 .*

Proof: We say that a line ℓ is *adapted* to a marked box M if it intersects both the side edges of the associated convex quad Q . Looking at Figure 3.2, we see that any line adapted to $t(M)$ is also adapted to M . Likewise, any line adapted to $b(M)$ is also adapted to M . Iterating, we see that any line adapted to any marked box in the semigroup orbit $\mathcal{O} = \langle r, b \rangle(M)$ is adapted to M . But any marked box in \mathcal{M} whose associated convex quadrilateral is contained in Q lies in \mathcal{O} . Applying this argument to $M = M_1$ we see that every line adapted to M_2 intersects both sides of S_1 . This result applies to the top and bottom lines of M_2 , which are adapted to M_2 . ♠

When M_1 is exactly as in Figure 2, the two segments of S_1 , namely \overline{cs} and \overline{au} both have their endpoints on opposite boundary components of the positive cone. The same thing therefore holds for an image of M under a positive diagonal matrix. But then any line which hits both edges of S_1 has non-negative slope. Hence the top line and bottom line of M_2 both have positive slope. This is a contradiction. Our proof of Theorem 1.1 is done.

5 Prisms and Bending

5.1 Triple Products of Flags

Suppose that $J = \{(p_k, \ell_k)\}$ is a triple of general position flags. We represent (p_k, ℓ_k) by a pair of vectors (P_k, L_k) where $P_k \cdot L_k = 0$. The *triple product* is defined as

$$\xi(J) = \frac{(P_1 \cdot L_2)(P_2 \cdot L_3)(P_3 \cdot L_1)}{(P_2 \cdot L_1)(P_3 \cdot L_2)(P_1 \cdot L_3)}. \quad (10)$$

This is an invariant that is independent of the way we represent our flags with vectors. Compare [FG]. If J' is a permutation of J then $\chi(J') = \chi(J)$ or $\chi(J') = 1/\chi(J)$, depending on whether we use an even or odd permutation.

Two triples of flags are equivalent under a projective transformation if and only if they have the same triple product. Indeed, when the triple of lines of the flag are not coincident – and this is generically the case – we can normalize a triple of flags as in Figure 5.1. This picture has 3-fold rotational symmetry. The invariant tells “how far out” the points are relative to the central triangle. Compare [S0, Figure 2.4.1]

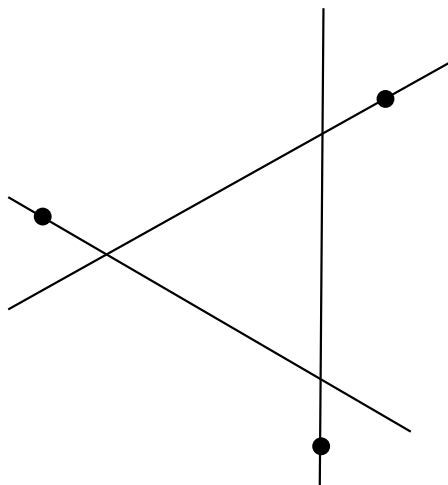


Figure 5.1 A normalized triple of flags

For the picture shown the triple product is negative. The positive case happens when the points are in the interiors of the edges of the central triangle. From this normalized structure we see that the only projective transformations stabilizing the generic flag is an order 3 rotation. Compare Lemma 3.1. Lemma 5.2 below discusses how polarities interact with triples of flags.

5.2 The Triple Product Invariant

We define the triple product of a marked box M to be the triple product of the flags

$$\tau(i(M)), \tau(t(M)), \tau(b(M)).$$

Here i, t, b are our three box operations and τ means “take the top flag associated to the marked box”. Our definition favors the top over the bottom. Were we to use the bottom flags, we would get the reciprocal.

Now we compute the triple product in terms of the box invariants. Suppose our marked box has box invariant $[(x, y)]$. Using the coordinates given in Figure 3.3, we compute

$$\chi(M) = -\frac{x(1-x)}{y(1-y)}. \quad (11)$$

Beautifully, this formula respects our equivalence relation

$$(x, y) \sim (1-x, 1-y).$$

This is a negative number. Since the box invariant for $i(M)$ is $[(1-y, x)]$ we see that $\chi(i(M)) = 1/\chi(M)$. This means that, up to taking reciprocals, $\chi(M)$ is independent of which M we take within a marked box orbit \mathcal{M} .

We define the *triple product invariant* of the Pappus modular group $\Lambda_{\mathcal{M}}$ to be

$$\chi(\Lambda_{\mathcal{M}}) = |\log(-\chi(M))|. \quad (12)$$

As we just said, this is well-defined independent of choices. Here we are using the fact that $|\log(r)| = |\log(1/r)|$. Here is a contour plot of the triple invariant as a function of the box invariant.

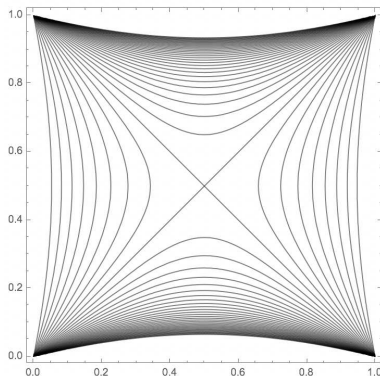


Figure 5.2 Level sets of the triple invariant

5.3 The Geometry of Prisms

Each marked box M in the orbit \mathcal{M} has a *foliated flat* f_M associated to it. The flat is the unique one that contains the geodesic γ_M . The foliation is by geodesics parallel to γ_M . This is the same picture we developed in the previous chapter. The flag f_M contains the order 2 fixed point p_M of the polarity that swaps M and $i(M)$, and γ_M is the geodesic through p_M .

As in the introduction, a *prism* is a triple of these flats corresponding to a triangle in the Farey triangulation. The three flats in the prism contain a triangle of geodesics in the Farey pattern which are pairwise one-end-asymptotic. Now we say further that the prism is actually foliated by such triangles of geodesics. The way this works is that the order 3 isometry which, on the boundary, permutes $i(M), t(M), b(M)$ cycles the flats in the prism and the triangles of which we speak are orbits of the foliating geodesics under this action. The triangle in the Farey pattern is one of these triangles, and the rest are like parallel displacements.

Our pattern of flats is really comprised of triangle-foliated prisms. The Farey pattern is obtained by taking the distinguished triangles within each foliated prism and snapping them together. Here is the lemma that underlies our bending phenomenon. By construction, all the foliated prisms within the same pattern are isometric to each other.

Lemma 5.1 *Suppose that M_1 and M_2 are two marked boxes having the property that $\chi(M_1) = \chi(M_2)$. Then the associated foliated prisms are isometric to each other via an isometry coming from a projective transformation.*

Proof: We can normalize by a projective transformation so that we have the same triple of flags. The foliated prism is determined just by the flag triple and not the underlying marked box. ♠

As a corollary, the foliated prisms associated to the Pappus modular groups Λ_1 and Λ_2 are all isometric to each other if $\chi(\Lambda_1) = \chi(\Lambda_2)$. So, if we vary the Pappus modular group and keep the triple product invariant the same, the geometry of the individual foliated prisms does not change. Only their relative geometry changes. This is our bending phenomenon.

What is happening as we move through a family of Pappus modular groups with the same triple invariant is that the distinguished triangles in each prism are changing. They are moving up and down the prism. Put

a better way, the associated order 2 fixed points are moving up and down the prism. Once we have one prism we get the adjacent ones by reflecting isometrically across these order 2 points. As the fixed points move, the geometric relation between a prism and its neighbor changes. This seems to me similar to doing an earthquake or a bend in the real hyperbolic setting. See [T] and [P]. Compare also [FG]. This is what I mean about a change in the geometry of one prism relative to an adjacent one.

5.4 The Triangles within a Prism

Suppose now we have two representations with the same triple invariant. One might wonder whether the associated geodesic triples in the Farey patterns are also isometric. Generically this is not the case. To prove this we need a preliminary lemma.

Lemma 5.2 *Let J be a triple of flags with triple invariant not equal to ± 1 . Then there are exactly three polarities which maps a triple of flags to itself. Each one permutes the flags by an odd permutation.*

Proof: Let Δ be the standard polarity. We let $J' = \Delta(J)$. The vectors representing the points and lines of J' can be taken to be the same as those representing the points and lines of J . All that has happened is that the interpretations of these vectors changes. If V formerly represented 1-dimensional subspace, then V is now a linear functional representing V^\perp .

For this reason, $\chi(J') = 1/\chi(J)$. If we permute the triple of flags in J' by an odd permutation we get a new triple J'' with $\chi(J'') = 1/\chi(J') = \chi(J)$. But then there is a projective transformation T such that $T(J) = J''$. But then, $\Delta \circ T(J) = \Delta(J'')$. This last triple is the same as the triple J but with the flags permuted by an odd permutation.

Our duality is $\psi = \Delta \circ T$. Note that $\psi^2(J) = J$ which means that ψ^2 is a projective transformation whose order is either 1 or 3. When we apply ψ twice, we are applying the same odd permutation, so ψ^2 acts as the identity permutation on the flags of J . Hence ψ^2 is the identity. Hence ψ is a polarity. Once we have one ψ we can get two more by composing ψ with one of the order 3 projective transformations which cycle the flags of J . ♠

Now we answer the question about the geometry of the triangles within a foliated prism.

Lemma 5.3 *If the triple product of the Pappus modular group is nonzero then each triangle in the prism foliation has at most one other triangle in the same foliation it could be isometric to.*

Proof: Let γ_1 and γ_2 be two triangles in the foliation. Suppose that I is an isometry of X such that $I(\gamma_1) = \gamma_2$. Since each geodesic of γ_j is contained in a unique flat, we see that I preserves our triple of flats. But then I stabilizes the triple of flags defining the triple of flats. This forces I to be one of 6 isometries determined by the flag, either the identity, one of the two projective transformations of order 3, or one of the polarities from Lemma 5.2. But the orbit of γ_1 under this order 6 group consists of either one or two triangles. Hence there is at most one other choice for γ_2 . ♠

Let me give another proof of Lemma 5.3. A polarity which preserves a flat must act as an order 2 rotation of that flat about some point. The reason is that the duality swaps \mathbf{P} and \mathbf{P}^* and therefore reverses the directions of all the singular geodesics in the flat. This forces the linear part of the isometry to be an order 2 rotation. But then there must be some fixed point in the flat as well. So, a polarity from Lemma 5.2 acts as an order 2 rotation about a fixed point in the flat that it stabilizes. In this way we see that each prism has 3 special points in it, one per flat. We call these points the *inflection points* of the prism. One of the triangles in the foliation contains the three inflection points, and the remaining triangles are at some distance from them. The distance to the inflection points is an isometry invariant of the triangle. For each positive distance d there are exactly two triangles in the foliation that are d away from the inflection points.

5.5 The Character Variety

The *character variety* is the space of Pappus modular groups modulo conjugation. The conjugation can be by isometries coming from projective transformation or by those coming from dualities.

To specify an element of the character variety, we choose a marked box orbit. There are 2 marked box invariants associated to this orbit, namely $[(x, y)]$ and $[(1 - y, x)]$. These invariants correspond to 4 points in the open unit square:

$$(x, y), \quad (1 - x, 1 - y), \quad (1 - y, x), \quad (y, 1 - x).$$

These can also be described as $\{\rho^k((x, y)) \mid k = 0, 1, 3, 4\}$ where ρ is the order 4 rotation fixing $(1/2, 1/2)$.

It is also worth mentioning that there is a projective transformation which maps the box with invariant $[(x, y)]$ to the box with invariant $[(y, x)]$ but switches the top edge and the bottom edge. This projective transformation does not completely respect the markings of the box but the only thing it does is switch the top and the bottom. The two Pappus modular groups are the same after we change the names of the generators. We will consider the two *representations* distinct.

This is all the symmetries we have. So, the character variety is an open cone: the quotient $C = (0, 1)/\langle \rho \rangle$. Referring to Figure 5.2, one can take a fundamental domain for the cone to be the upper quadrant shown in Figure 5.3. One gets the cone by identifying the bounding diagonals in Figure 5.3. Reflection in the vertical midline is an involution which, as mentioned above, preserves the Pappus modular group but changes the representation.

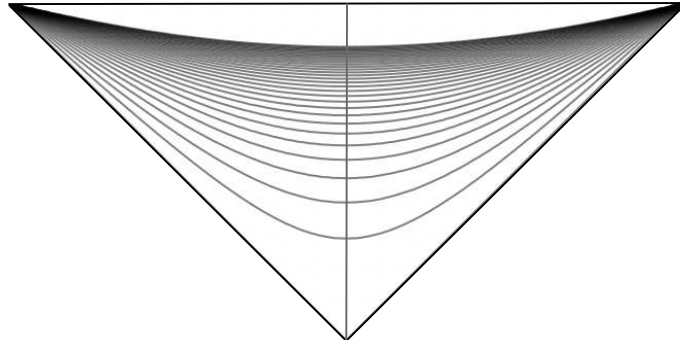


Figure 5.3 The character variety and its triple product foliation

The cone point of C , the point $(1/2, 1/2)$, corresponds to the Fuchsian representation, the one associated to a maximally symmetric marked box. The diagonal edges of slope ± 1 , which glue together in C to make a single segment, correspond to representations which have an extra symmetry. The picture in Figure 1.2 comes from a point in this segment.

Each prism associated to a generic Pappus modular group has an order 6 isometry group. An index 2 cyclic subgroup, the one given by Lemma 3.1, is in the Pappus modular group. The other elements typically are not: They act as involutions on the flag triple but not of the marked boxes. In the next section we will discuss the way an extra symmetry arises in some of the representations.

5.6 Axial Pappus Representations

The remaining level sets of the triple invariant are open segments. Each of these open segments has a canonical *axis point* on the vertical axis in Figure 5.3. We call the corresponding representations *axial representations*. If we fix the triple invariant, then the axial representation in the level set is a distinguished origin of the level set. I might conjecture that quantities like e.g. the Hausdorff dimension of the limit set vary monotonically as one moves along one of these level sets away from the axis point. I say that I *might* conjecture because I have not investigated this at all.

Lemma 5.4 *For an axial representation, the inflection points of the prisms are contained in the geodesics of the Farey pattern.*

Proof: For the axial representations, half the marked boxes in the orbit have box invariant $[(x, 1/2)]$ and the other half have box invariant $[(1/2, x)]$. In this case, there is a projective transformation which maps M to $i(M)$ and swaps the top and bottom. Composing this with the polarity that maps $i(M)$ to M , we get a polarity ρ that preserves M and swaps the top and the bottom. The polarity ρ preserves the marked box orbit (up to switching tops and bottoms) and therefore both the Farey pattern and the pattern of flats. At the same time ρ preserves the triple of flags associated to M and thus is one of the extra isometries of the corresponding prism. Since ρ preserves the Farey pattern and fixes one of the inflection points of a prism, we see that this inflection lies in the Farey pattern. But then this is true for all the inflection points by symmetry. ♠

Lemma 5.5 *For an axial representation, the inflection points of the prisms are the fixed points of the order 2 elements of the Pappus modular group.*

Proof: By the previous lemma, each inflection point lies in the same geodesic of the Farey pattern as an order 2 fixed point. If this lemma is false, we would have two order 2 isometries of the Farey pattern fixing distinct points in the same geodesic. The square of the product would generate an infinite subgroup of isometries of the Farey pattern stabilizing one of the prisms. This contradicts Lemma 5.2. ♠

5.7 Inflection Lines and Fixed Points

Each prism has a triple of distinguished singular lines. These are the lines perpendicular to the triangles in the triangle foliation and containing the inflection points. We call these the *inflection lines*.

Lemma 5.6 *For any Pappus modular representation, the order 2 fixed points lie on the inflection lines. The inflection lines in the same flat, defined relative to adjacent prisms which contain it, coincide.*

Proof: This is a calculation. We work with respect to the marked box M shown in Figure 3.3. To avoid a tedious accounting of the points and lines which I would probably do incorrectly anyway, let me be a bit vague about which matrix I am computing.

Let δ be the polarity swapping M and $i(M)$. Let Σ denote the set of 6 polarities associated to the prisms associated to M and $i(M)$. Then we have 12 possible linear transformations of the form $\delta \circ \sigma$ or $\sigma \circ \delta$ where $\sigma \in \Sigma$. One of these, which we call T , has the action

$$\begin{aligned} T(t) = t, \quad T(b) = b, \quad T([1 : 0 : 0]) = [1 : 0 : 0], \quad T([1 : 1 : 2]) = [0 : 1 : 0], \\ [1 : 0 : 0] = \overline{su} \cap \overline{ac}, \quad [1 : 1 : 2] = \overline{sa} \cap \overline{uc}, \quad [0 : 1 : 0] := \overline{sc} \cap \overline{ua}. \end{aligned}$$

We compute that

$$T\alpha \begin{bmatrix} \frac{-1+x+y}{x-y} & \frac{-1+3x+y-4xy}{x-y} & \frac{1-2x-y+2xy}{x-y} \\ 0 & 1 & 0 \\ 0 & 2 & -1 \end{bmatrix} \quad (13)$$

Here α is a constant which makes $\det(T) = 1$. The eigenvalues for T/α are

$$1, \quad -1 \quad \frac{-1+x+y}{x-y}.$$

The corresponding eigenvectors represent the points $t, b, [1 : 0 : 0]$. Notice that T acts as an isometry on the flat determined by the top and bottom flag of M . The eigensystem calculation identifies T as a translation along the singular lines which limit in one direction to $[1 : 0 : 0]$. This is only possible if the fixed point of δ and the inflection point are on the same singular line. ♠

Remark: Here is some speculation. We fix a prism P and restrict our attention to those Pappus modular groups which have P as part of the pattern of flats. This gives us instances of all the representations with a certain triple invariant. As we range over the level set, the order 2 fixed points of the associated groups sweep out the inflection lines.

We choose 3 points in P that are permuted by the order 3 symmetry g of P and then look at the group generated by g and the definite polarities which fix these 3 points. If we choose the points to be in the inflection lines, we recover the Pappus modular groups we have been talking about. If we pick these points off the inflection lines, we get something new. Perhaps this is an alternate description of the additional family of groups found in [BLV].

5.8 An Attempt at a Pleated Plane

Let me explain at least one way to fill in $\Gamma_{\mathcal{M}}$ to get something like a pleated surface. Consider a Farey triangle τ in this pattern. Let $\gamma_1, \gamma_2, \gamma_3$ be the corresponding unoriented geodesics in X . There is a distinguished point $p_j \in \gamma_2$. This is the point fixed by the polarity associated to γ_j .

Lemma 5.7 *The points p_1, p_2, p_3 define a canonical center of symmetry c that is invariant under the stabilizer of τ in $\Lambda_{\mathcal{M}}$.*

Proof: Since X has non-positive curvature, the following iterative construction will limit to a point. Let ξ_0 be the triangle with vertices p_1, p_2, p_3 . In general let ζ_{k+1} be the triangle whose vertices are the midpoints of the geodesics connecting the vertices of ζ_k .

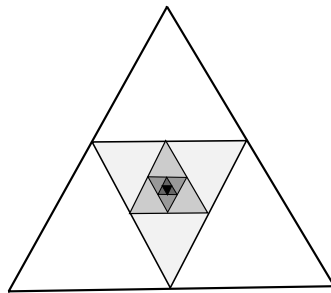


Figure 4.4: An iterative construction of the center point

Figure 4.4 shows the corresponding Euclidean construction. Then the sequence $\{\zeta_k\}$ shrinks to a point. This is our point c . ♠

Remark: Given that X has non-positive curvature, there are probably many other constructions of a canonical center point. For example, one could take c to be the unique point which minimizes the sum of the squares of the distances to p_1, p_2, p_3 .

Now that we have c , we create a *wedge* w_j by geodesically coning γ_j to c . The union $w_1 \cup w_2 \cup w_3$ is a piecewise analytic “ideal triangle” whose boundary is τ . These filled in ideal triangles snap together to give a piecewise analytic topological disk $\Pi_{\mathcal{M}}$. The analytic pieces are all wedges. They meet along geodesic rays and along geodesics. So, the disk $\Pi_{\mathcal{M}}$ is a piecewise analytic disk with geodesic pleats.

Remarks:

- (1) The disjointness result I proved above does not imply that the pleated surface is embedded, but I strongly suspect that it is.
- (2) I don’t really have a good understanding of the geometry of a wedge. In general, if you geodesically cone a geodesic γ to a point $c \in X - \gamma$ you get a surface whose geometry ranges from Euclidean (in case c and γ lie in a common flat) to hyperbolic (in case c and γ lie in a common totally geodesic copy of \mathbf{H}^2). In the case which arises for a general Pappus modular group, the geometry is probably strictly in between these. For the symmetric case the wedges are hyperbolic, and they fit together to make a totally geodesic copy of \mathbf{H}^2 . As we move away from the symmetric case, I think that the geometry gradually moves away from being purely hyperboilc. I have not really done any calculations about this, however.
- (3) The approach I take here is quite elementary though perhaps it is not the best approach. Anna Wienhard pointed out to me that cones in higher rank are pretty hard to control geometrically, and she suggested to me that perhaps the approach taken in [DR] might work better.
- (4) One can make this construction for each triangle in a foliated prism and then take the union to get a kind of foliated 3-manifold-with-boundary. Something tells me that there is a better way to fill in these prisms, but I have not yet thought this through.

6 References

- [Bar] T. Barbot, *Three dimensional Anosov Flag Manifolds*, Geometry & Topology (2010)
- [BLV], T. Barbot, G. Lee, V. P. Valerio, *Pappus's Theorem, Schwartz Representations, and Anosov Representations*, Ann. Inst. Fourier (Grenoble) **68** (2018) no. 6
- [BCLS] M. Bridgeman, D. Canary, F. Labourie, A. Samburino, *The pressure metric for Anosov representations*, Geometry and Functional Analysis **25** (2015)
- [DR] C. Davalo and J. M. Riestenberg, *Finite-sided Dirichlet domains and Anosov subgroups*, arXiv 2402.06408 (2024)
- [FG]. V. Fock and A. Goncharov, *Moduli Spaces of local systems and higher Teichmuller Theory*, Publ. IHES **103** (2006)
- [G] W. Goldman, *Convex real projective structures on compact surfaces*, J. Diff. Geom. **31** (1990)
- [GW] O. Guichard, A. Wienhard, *Anosov Representations: Domains of Discontinuity and applications*, Invent Math **190** (2012)
- [Hit] N. Hitchin, *Lie Groups and Teichmuller Space*, Topology **31** (1992)
- [KL] M. Kapovich, B. Leeb, *Relativizing characterizations of Anosov subgroups, I (with an appendix by Gregory A. Soifer)*. Groups Geom. Dyn. **17** (2023)
- [Lab] F. Labourie, *Anosov Flows, Surface Groups and Curves in Projective Spaces*, P.A.M.Q **3** (2007)
- [P] R. Penner, *The Decorated Teichmuller Theory of punctured surfaces*, Comm. Math. Pys. **113** (1987)
- [S0] R. E. Schwartz, *Pappus's Theorem and the Modular Group*, Publ. IHES (1993)
- [T] W. Thurston, *The Geometry and Topology of Three Manifolds*, Princeton University Notes (1978)